lncRNA EZR-AS1 knockdown represses proliferation, migration and invasion of cSCC via the PI3K/AKT signaling pathway

DI LU[1], LINGLING SUN[2], ZHENGJUN LI[3] and ZHEN MU[4]

Departments of [1]Dermatology and [2]Oncology, Zibo First Hospital, Zibo, Shandong 255200; [3]Department of Dermatology, Qilu Hospital of Shandong University, Ji'nan, Shandong 250012; [4]Department of Dermatology, The Second Affiliated Hospital of Shandong First Medical University, Tai'an, Shandong 271000, P.R. China

Received June 18, 2020; Accepted October 21, 2020

DOI: 10.3892/mmr.2020.11714

Abstract. Although long non-coding RNAs (lncRNAs) have been implicated in various human cancer types, the role of lncRNA ezrin antisense RNA 1 (EZR-AS1) in cutaneous squamous cell carcinoma (cSCC) remains unclear. The present study aimed to investigate the effect of lncRNAEZR-AS1 on cSCC and identify the underlying molecular mechanisms. EZR-AS1 expression was measured in cSCC tissue and cells detected using reverse transcription-quantitative PCR. Gain-of-function assays were performed in A431 cells, which have a relatively low expression of EZR-AS1, while loss-of-function assays were performed in SCC13 and SCL-1 colon cancer cells, which have a relatively high expression of EZR-AS1. Cell viability, proliferation, migration, invasion and apoptosis were assessed using MTT, plate cloning, wound healing, Transwell and flow cytometry assays, respectively. EZR-AS1 mRNA expression levels were significantly upregulated in cSCC tissues and cells compared with adjacent healthy tissues and HaCaT cells, respectively. Compared with the small interfering RNA (si)-negative control (NC) group, si-EZR-AS1 significantly inhibited SCC13 and SCL-1 cell proliferation, migration and invasion, but promoted cell apoptosis. By contrast, compared with the pc-NC group, EZR-AS1 overexpression significantly enhanced A431 cell proliferation, migration and invasion, but inhibited cell apoptosis. Moreover, focal adhesion kinase (FAK) was identified as a target of EZR-AS1, and EZR-AS1 knockdown significantly decreased FAK expression compared with the si-NC group. Moreover, EZR-AS1 knockdown significantly downregulated the protein expression levels of phosphorylated (p)-PI3K/PI3K and p-AKT/AKT in cSCC cells compared with the si-NC group. The PI3K agonist 740Y-P significantly reversed si-EZR-AS1-mediated effects on SCC13 and SCL-1 cell proliferation, migration, invasion and apoptosis. In conclusion, the present study demonstrated that si-EZR-AS1 inhibited cSCC cell proliferation, migration and invasion, and promoted cell apoptosis, potentially via regulating the PI3K/AKT signaling pathway. Therefore, the present study provided novel insights into the diagnosis and treatment of cSCC.

Correspondence to: Professor Zhen Mu, Department of Dermatology, The Second Affiliated Hospital of Shandong First Medical University, 706 Taishan Street, Tai'an, Shandong 271000, P.R. China
E-mail: sdzbldsll@163.com

Key words: long non-coding RNA, ezrin antisense RNA 1, cutaneous squamous cell carcinoma, PI3K/AKT

Introduction

Cutaneous squamous cell carcinoma (cSCC) is a malignant tumor that originates from epidermal or appendage keratinocytes (1). cSCC primarily occurs in the elderly population in light-exposed areas, including the scalp, face and back of the hands (2). cSCC is not life threatening, but if left untreated can grow larger or spread to other organs causing serious complications, local lymph node metastases and distant metastases (3). Previous studies have reported that cSCC accounts for ~20% of all skin malignant tumors (4,5). For the majority of patients with cSCC, a good prognosis can be achieved if the lesion is completely removed by surgery. However, for patients who cannot undergo surgery or have metastatic disease, radiotherapy and chemotherapy are common treatment strategies used. Although radiotherapy and chemotherapy have been widely used for the treatment of cSCC, these strategies are not recommended due to their side effects and inconsistent therapeutic effects (6,7). Targeted molecular therapy has become a recent trend in cSCC therapy (8), thus investigating the molecular mechanism underlying cSCC progression is important for the identification of novel therapeutic targets.

Long non-coding RNAs (lncRNAs) are non-coding RNAs that are >200 nucleotides in length (9). Previous studies have demonstrated that lncRNAs serve important roles in numerous biological functions, including the dose compensation effect, epigenetic regulation, cell cycle regulation and cell differentiation regulation (10,11). In recent years, lncRNAs have become a focus of research and increasing evidence has demonstrated that lncRNAs regulate human cancer cell proliferation, apoptosis, migration and invasion (12,13). Recent research has reported that certain lncRNAs that might be involved in tumorigenesis and development are differentially expressed in tumor tissues compared with healthy tissues (14). lncRNA ezrin antisense RNA 1 (EZR-AS1) is a natural antisense

lncRNA transcribed from the opposite strand at the EZR gene locus, which is located on chromosome 6q25.3, with a length of 362 bp (15,16). Ghaffari *et al* (17) demonstrated that EZR inhibition impedes breast cancer cell migration and lymph node metastasis. Xie *et al* (18,19) reported that EZR expression is related to poor overall survival of patients with esophageal squamous cell carcinoma (ESCC). Furthermore, EZR-AS1 knockdown significantly suppresses human breast cancer MCF7 and MDA-MB-231 cell proliferation and cell cycle progression (20). Zhang *et al* (21) reported that EZR-AS1 knockout significantly inhibited ESCC cell migration, reduced tumor volume and weight, and decreased the number of metastatic lymph nodes in mice (21). However, the biological function of lncRNA EZR-AS1 in cSCC cells and the underlying molecular mechanism are not completely understood.

PI3K/AKT is a classical signaling pathway that serves a vital role in carcinogenesis (22). The PI3K/AKT signaling pathway regulates a variety of physiological functions, including cell survival, proliferation, migration, invasion and protein translation (23,24). More importantly, it has been reported that the PI3K/AKT signaling pathway critically controls cSCC cell survival, and molecular alterations to the signaling pathway, including phosphorylation of PI3K and AKT, have been widely reported in cancer (22,25). Liu *et al* (15) have indicated that silencing of lncRNA EZR-AS1 inhibits proliferation, invasion, and migration of colorectal cancer cells through blocking TGF-β signaling. However, whether EZR-AS1 could regulate the PI3K/Akt signaling pathway in the progression of cSCC remains unclear.

In the present study, we aimed to investigate whether lncRNA EZR-AS1 promote the progression of cSCC by regulating the PI3K/Akt signaling pathway, thereby further revealing the regulatory role of lncRNA EZR-AS1 in cSCC and helping to find new targets for the cSCC therapy.

Materials and methods

Clinical sample collection. A total of 66 cSCC tissues and healthy adjacent non-cancerous tissues (1-2 cm from cSCC tissues) were obtained from patients with cSCC (37 males and 29 females; age range, 25-79 years) who underwent surgery at the Second Affiliated Hospital of Shandong First Medical University (Tai'an, China) between January 2014 and September 2019. All tissues were immediately frozen in liquid nitrogen and stored at -80˚C until further analysis. Written informed consent was obtained from all patients. The present study was approved by the Ethics Committee of The Second Affiliated Hospital of Shandong First Medical University.

Cell culture. CSCC cell lines (SCL-1, SCC13, A431 and HSC-5) and a human immortalized keratinocytes line (HaCaT; cat. no. CC-Y1177) were obtained from EK-Biosciences. Cells were cultured in RPMI-1640 (Gibco; Thermo Fisher Scientific, Inc.) supplemented with 10% FBS (Sigma-Aldrich; Merck KGaA) in a humidified environment with 5% CO_2 at 37˚C. The medium was changed every 2-3 days.

Cell transfection. At 70-80% confluence, SCC13, SCL-1 and A431 cells were inoculated into a 6-cm culture dish. SCC13 and SCL-1 cells were divided into the following groups: i) Control, untreated; ii) si-NC, transfected with 0.5 μg siRNA NC (scrambled control); iii) si-EZR-AS1-1, transfected with 0.5 μg siRNA-EZR-AS1-1; iv) si-EZR-AS1-2, transfected with 0.5 μg siRNA-EZR-AS1-2; v) pc-NC, transfected with 1 μg pcDNA3.1 NC (empty vector; Invitrogen; Thermo Fisher Scientific, Inc.); vi) pc-FAK, transfected with 1 μg pcDNA3.1-FAK (Invitrogen; Thermo Fisher Scientific, Inc.); and vii) pc-FAK + si-EZR-AS1-1, co-transfected with 1 μg pc-FAK and 0.5 μg si-EZR-AS1-1. All siRNAs were purchased from Shanghai GenePharma, Co., Ltd., whereas plasmids were from Invitrogen (Thermo Fisher Scientific, Inc.). A431 cells were divided into three groups: i) Control, untreated; ii) pc-NC, transfected with 1 μg pcDNA3.1 NC; and iii) pc-FAK, transfected with 1 μg pcDNA3.1-FAK.

Cells were transfected using Lipofectamine® 2000 (Invitrogen; Thermo Fisher Scientific, Inc.). At 48 h post-transfection, si-NC- and si-EZR-AS1-1-transfected SCC13 cells were cultured in RPMI-1640 containing 20 μM 740Y-P (a PI3K agonist; MedChem Express) for 2 h at 37˚C to establish the following groups: i) Control, si-NC-transfected SCC13 cells; ii) 740-YP, si-NC-transfected SCC13 cells treated with 740Y-P; iii) si-EZR-AS1-1, si-EZR-AS1-1 transfected SCC13 cells; and iv) 740-YP + si-EZR-AS1-1, si-EZR-AS1-1 transfected SCC13 cells treated with 740Y-P. After 48-h transfection at 37˚C, cells were used for subsequent experiments. The sequences of the EZR-AS1 siRNAs were as follows: i) si-EZR-AS1-1, 5'-AAA UAAUACUACAAUUAAA-3'; ii) si-EZR-AS1-2, 5'-UUU AAUUGUAGUAUUAUUU-3'; and iii) si-NC, 5'-UUCUCC GAACGUGUCACGUTT-3'.

Reverse transcription-quantitative PCR (RT-qPCR). Total RNA was extracted from of cells (SCL-1, SCC13, A431, HSC-5 and HaCaT cells) and tissues (healthy and cSCC tissues) using TRIzol® reagent (Invitrogen; Thermo Fisher Scientific, Inc.). Total RNA was reverse transcribed into cDNA using the PrimeScript™ RT Reagent Kit (Takara Bio, Inc.). Reverse transcription was performed at 16˚C for 30 min, 42˚C for 30 min and 85˚C for 5 min. Subsequently, SYBR® Premix Ex Taq™ (Takara Biotechnology Co., Ltd.) was used to examine the expression of lncRNA and mRNA. qPCR was performed using the following thermocycling conditions: 94˚C for 6 min; 35 cycles of 96˚C for 20 sec, 58˚C for 40 sec and extension at 72˚C for 2 min. The relative gene expression was determined using the $2^{-\Delta\Delta Cq}$ method (26). The following primers were used for qPCR: EZR-AS1 forward, 5'-CCCTCT CCAATGAAGCCTCTC-3' and reverse, 5'-ACCGAAAAT GCCGAAACCAG-3'; EZR forward, 5'-TGATCACGCTGT AAGGCACA-3' and reverse, 5'-AGGCCTCATGTACCC CTCTT-3'; FAK forward, 5'-CTATGGTGAAGGAAGTCG GCTTGG-3' and reverse, 5'-TGTACTCTTGCTGGAGGC TGGTC-3'; and GAPDH forward, 5'-TCCTCTGACTTCAAC AGCGACAC-3' and reverse, 5'-CACCCTGTTGCTGTAGCC AAATTC-3'. mRNA expression levels were normalized to the internal reference gene GAPDH.

Western blotting. At 48 h post-transfection, total protein was extracted from cells from each group using a Total protein extraction kit (BestBio Science). Protein concentration was determined using a bicinchoninic acid kit (Abcam). Proteins (50 μg per lane) were separated by SDS-PAGE on 12%

gels and transferred to PVDF membranes. After blocking with 5% dry skimmed milk for 2.5 h at room temperature, the membranes were incubated with the primary antibodies overnight at 4˚C. The primary antibodies including PI3K (1:1,000; cat. no. 4257), phosphorylated (p)-PI3K (1:1,000; cat. no. 17366), AKT (1:1,000; cat. no. 4685), p-AKT (1:1,000; cat. no. 4060), FAK (1:1,000; cat. no. 13009), matrix metallopeptidase (MMP)-2 (1:1,000; cat. no. 40994), MMP-9 (1:1,000; cat. no. 13667), Bcl-2 (1:1,000; cat. no. 4223) and Bax (1:1,000, cat. no. 14796) and β-actin (1:1,000; cat. no. 4970). All primary antibodies were purchased form Cell Signaling Technology, Inc. Subsequently, the membranes were incubated with a horseradish peroxidase-conjugated goat anti-rabbit secondary antibody (1:1,000; cat. no. A0277; Beyotime Institute of Biotechnology) at room temperature for 45 min. Protein bands were visualized using electrochemiluminescent solution (Thermo Fisher Scientific, Inc.). Protein expression levels were semi-quantified using ImageJ software (version 1.8.0; National Institutes of Health).

LncRNA-EZR-AS1 binding prediction with LncTar. To predict the targeted mRNAs of lncRNA EZR-AS1, an ensemble classifier-based predictor, lncLocator (http://www.csbio.sjtu.edu.cn/bioinf/lncLocator/) was performed in this study. The operational process of lncLocator was conducted as previously described (27). Briefly, both k-mer features and high-level abstraction features generated by unsupervised deep models were used to construct four classifiers for support vector machine (SVM) and random forest (RF), respectively. A stacked ensemble strategy was then used to combine the four classifiers for final prediction results.

RNA immunoprecipitation (RIP) assay. The RIP assay was performed using the Magna RIP kit (EMD Millipore) to verify the binding relationship between EZR-AS1 and FAK. SCC13 and SCL-1 cells were lysed using RIP lysis buffer and then incubated with anti-FAK or anti-IgG antibodies overnight at 4˚C, followed by incubation with protein A magnetic beads at 4˚C for 4 h. The co-precipitated RNAs were isolated to detect the expression levels of EZR-AS1 and FAK via RT-qPCR.

Cell viability analysis. At 24, 48, 72 and 96 h, cell viability in each group was assessed by performing the MTT assay. Cells were seeded into a 96-well plate at a density of $5x10^3$ cells/well and cultured at 37˚C with 5% CO_2. Subsequently, 20 μl MTT solution (5 mg/ml; Sigma-Aldrich; Merck KGaA) was added to each well and incubated at 37˚C with 5% CO_2. Following incubation for 4 h, 150 μl DMSO was added to each well for 10 min with gentle agitation to dissolve the formazan crystals. Absorbance was measured at a wavelength of 570 nm using a microplate reader.

Plate cloning experiment. Cells in the logarithmic growth phase of each group were collected and seeded ($5x10^2$ cells/well) into 6-well plates. Cells were cultured for 14 days and the medium was changed every 2 to 3 days. After washing twice with PBS, cells were fixed with 4% formaldehyde for 15 min at 37˚C and stained with crystal violet for 10-20 min at room temperature. Following washing with distilled water, cell colonies were observed and counted using a light microscope (Carl Zeiss AG). Cell colonies were defined as cell clusters containing ≥50 cells. Images of the cell colonies were directly obtained using a camera.

Wound healing assay. Cells were seeded into a 6-well plate and cultured in RPMI-1640 supplemented with 10% FBS until the cells were grown to 100% confluence. A 10 μl pipette tip was used to create a scratch wound in the cell monolayer. The medium was aspirated to remove the detached cells. Serum-free medium (Gibco; Thermo Fisher Scientific, Inc.) was added to the 6-well plate. At 0 and 48 h, cell migration was observed using an inverted light microscope (magnification, x100; Carl Zeiss AG) and photographed using a Cybershot camera (Sony Corporation). Image-Pro Plus 6.0 software (Media Cybernetics, Inc.) was used to quantify the wound distance at 0 and 48 h. The percentage of gap closure was used as an indicator of cell migration. The percentage of gap closure is calculated as (average distance at 0 h-average distance at 48 h)/(average distance at 0 h) x100%.

Transwell invasion assay. At 48 h post-transfection, cells were trypsinized and resuspended in serum-free medium. Matrigel™ (BD Biosciences) was used to precoat the membrane of the upper chambers at 37˚C for 2 h. Cells ($1x10^5$) in serum-free medium were plated into the upper chamber and medium containing 15% FBS was plated into the lower chamber. Following incubation at 37˚C for 24 h, cells were rinsed with PBS, fixed with 4% paraformaldehyde at room temperature for 15 min and stained with 0.1% crystal violet at 37˚C for 30 min. Invading cells were observed in five randomly selected fields of view using an light microscope (magnification, x200; Carl Zeiss AG).

Cell apoptosis assay. Cell apoptosis was detected via flow cytometry using the Annexin V-PI kit (Invitrogen; Thermo Fisher Scientific, Inc.). Briefly, cells were cultured at 37˚C with 5% CO_2 for 48 h. Cells were collected by centrifugation at 850 x g for 5 min at room temperature. A total of $1x10^5$ cells were incubated with Annexin V in the dark at 4˚C for 20 min and then 10 μl PI in the dark for 15 min. Cell apoptosis was acquired using a FACSCalibur flow cytometer (BD Biosciences) and analyzed on FlowJo 7.0 software (FlowJo LLC). The sum of early apoptotic cells and late apoptotic cells was assessed.

Statistical analysis. Data are presented as the mean ± SD of at least three independent experiments. Statistical analyses were performed using GraphPad Prism software (version 7.0; GraphPad Software, Inc.). Comparisons between two matched groups were analyzed using paired Student's t-tests. Comparisons among multiple groups were analyzed using one-way ANOVA followed by Tukey's post hoc test. The data presented in Table I was analyzed using the χ^2 test. $P<0.05$ was considered to indicate a statistically significant difference. Experiments were repeated at least three times.

Results

lncRNA EZR-AS1 expression is upregulated in cSCC cells. EZR-AS1 mRNA expression levels were significantly

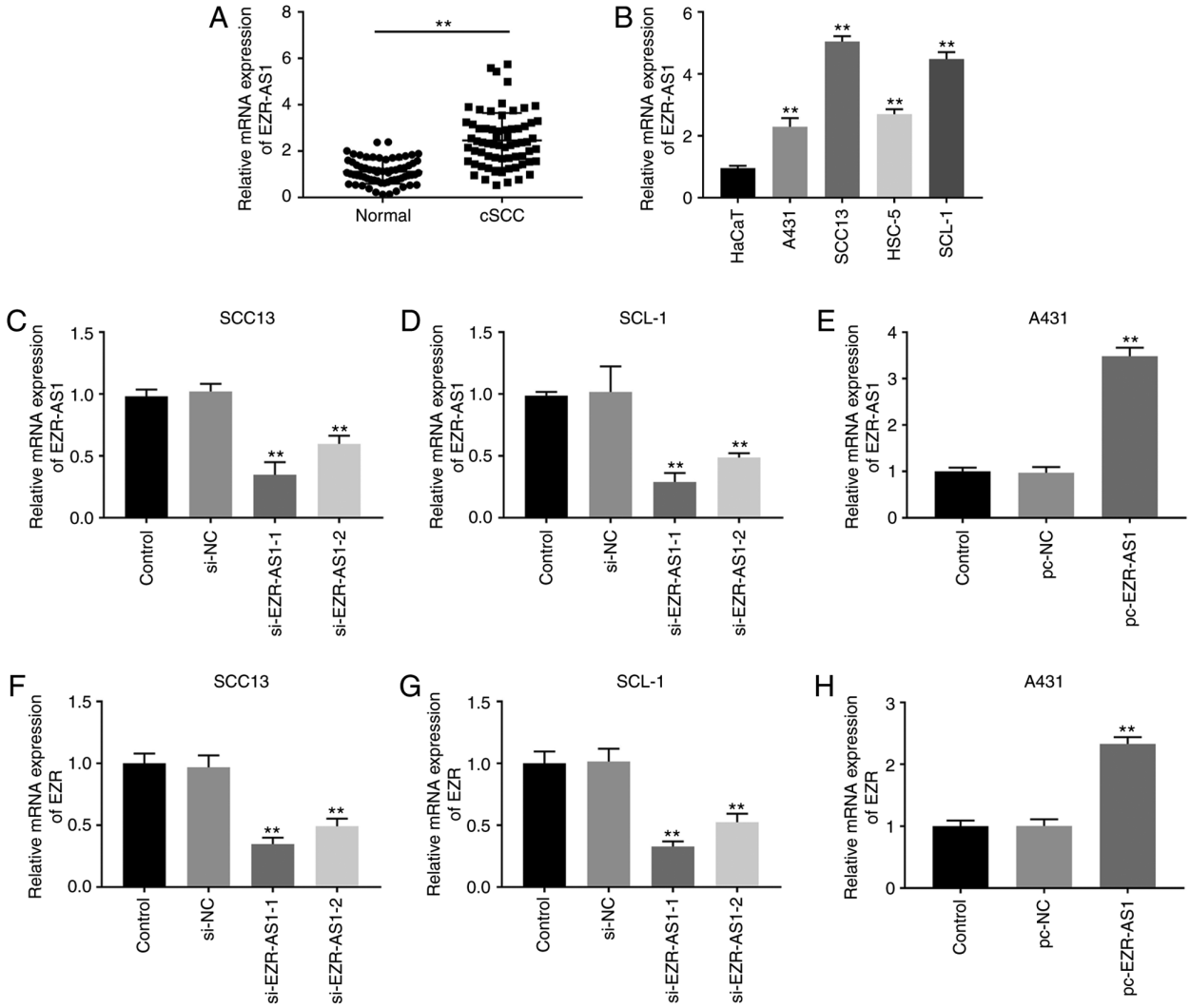

Figure 1. Long non-coding RNA EZR-AS1 expression is upregulated in cSCC cells. (A) EZR-AS1 mRNA expression levels in cSCC tissues and healthy adjacent tissues. (B) EZR-AS1 mRNA expression levels in cSCC cell lines (A431, SCC13, HSC-5 and SCL-1) and the human immortalized keratinocyte cell line (HaCaT). Transfection efficiency of si-EZR-AS1-1 and si-EZR-AS1-2 in (C) SCC13 and (D) SCL-1 cells. (E) Transfection efficiency of pc-EZR-AS1 in A431 cells. EZR mRNA expression levels in si-EZR-AS1-1- and si-EZR-AS1-2-transfected (F) SCC13 and (G) SCL-1 cells. (H) EZR mRNA expression levels in pc-EZR-AS1-transfected A431 cells. **P<0.01 vs. HaCaT, si-NC or pc-NC. EZR-AS1, ezrin antisense RNA 1; cSCC, cutaneous squamous cell carcinoma; si, small interfering RNA; NC, negative control.

increased in cSCC tissues compared with adjacent healthy tissues (P<0.01; Fig. 1A). EZR-AS1 expression levels in cSCC cell lines (A431, SCC13, HSC-5 and SCL-1) and the human immortalized keratinocyte cell line (HaCaT) were measured. EZR-AS1 expression levels were significantly increased in cSCC cell lines compared with HaCaT cells, especially in SCC13 and SCL-1 cells (P<0.01; Fig. 1B). In addition, based on the median expression level (2.33) of EZR-AS1, patients with cSCC were divided into two groups: i) High expression; and ii) low expression. The associations between EZR-AS1 expression and clinicopathological characteristics are presented in Table I. EZR-AS1 expression was significantly associated with histopathological grade and lymph node metastasis (P<0.05), but there was no significant association with age and sex (P>0.05).

si-EZR-AS1 inhibits cSCC cell proliferation. To further investigate the effect of EZR-AS1 on cSCC progression, SCC13 and SCL-1 cells were transfected with si-EZR-AS1 or si-NC, and A431 cells were transfected with pc-EZR-AS1 or pc-NC. In SCC13 and SCL-1 cells, EZR-AS1 expression was significantly decreased in the si-EZR-AS1-1 and si-EZR-AS1-2 groups compared with the si-NC group, especially in the si-EZR-AS1-1 group (P<0.01; Fig. 1C and D). In A431 cells, EZR-AS1 expression in the pc-EZR-AS1 group was significantly higher compared with the pc-NC group (P<0.01; Fig. 1E). Similar results were observed for EZR expression. In SCC13 and SCL-1 cells, EZR mRNA expression levels in the si-EZR-AS1-1 and si-EZR-AS1-2 groups were significantly lower compared with the si-NC group (P<0.01; Fig. 1F and G). In A431 cells, EZR mRNA expression levels in the pcEZR-AS1 group were significantly increased compared with the pc-NC group (P<0.01; Fig. 1H). Subsequently, MTT and plate cloning assays were performed to detect the effects of EZR-AS1 on cSCC cell proliferation. The MTT and plate cloning assay results indicated that EZR-AS1 knockdown significantly decreased cell viability and colony formation compared with the si-NC group, whereas EZR-AS1 overexpression

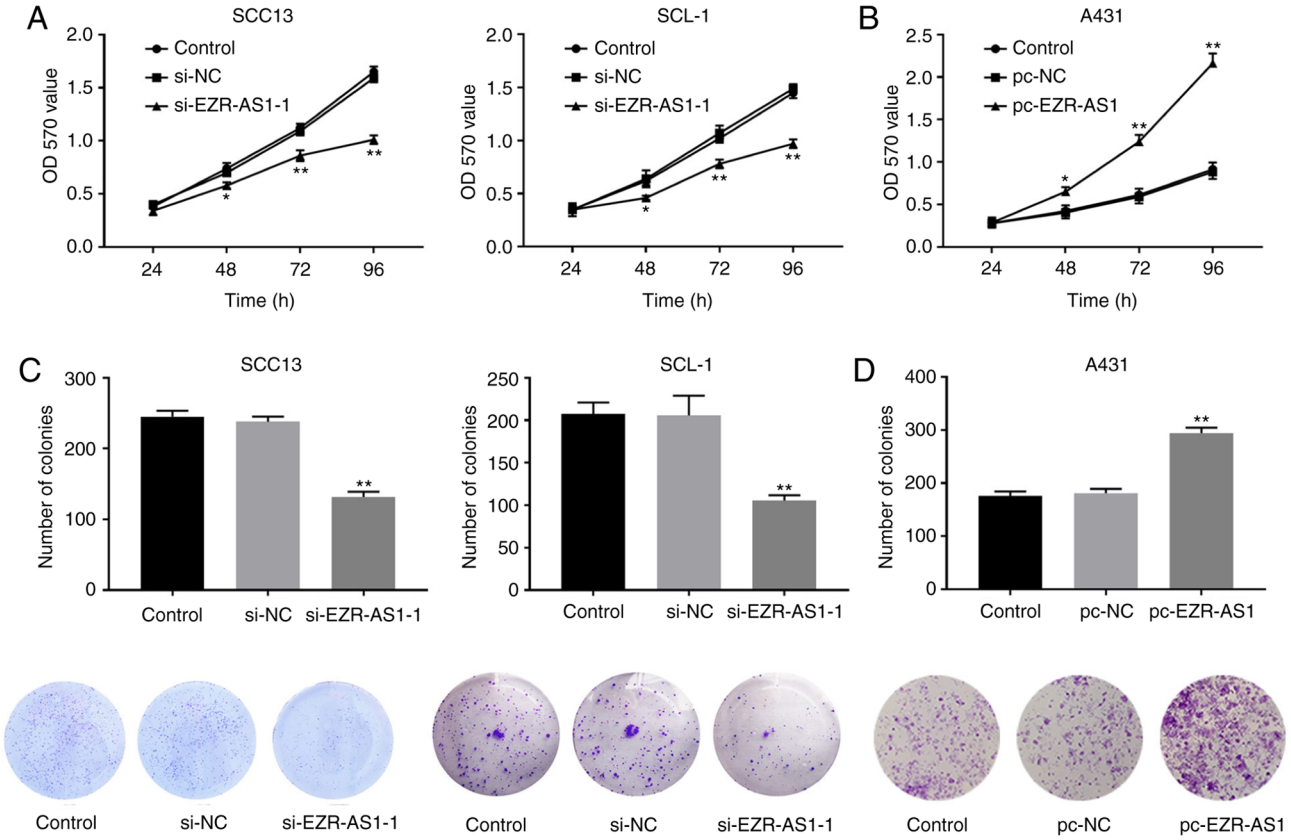

Figure 2. si-EZR-AS1 inhibits cutaneous squamous cell carcinoma cell proliferation. The MTT assay was performed to assess (A) SCC13, SCL-1 and (B) A431 cell proliferation. The plate cloning assay was performed to assess (C) SCC13, SCL-1 and (D) A431 cell colony formation. Magnification, x40. *P<0.05 vs. si-NC or pc-NC. **P<0.01 vs. si-NC or pc-NC. si, small interfering RNA; EZR-AS1, ezrin antisense RNA 1; si, small interfering RNA; NC, negative control; OD, optical density.

Table I. Correlation between EZR-AS1 expression and clinicopathological parameters.

		EZR-AS1 expression		
Parameters	Total	Low	High	P-value
Age, years				0.445
<55	30	13	17	
≥55	36	19	17	
Sex				0.457
Male	37	20	17	
Female	29	13	16	
Lymph node metastasis				0.037[a]
Present	22	7	15	
Absent	44	26	18	
Histopathological grade				0.041[a]
Well to moderate	42	25	17	
Poor	24	8	16	

EZR-AS1, ezrin antisense RNA 1. [a]P<0.05.

significantly increased cell viability and colony formation compared with the pc-NC group (all P<0.01; Fig. 2). Therefore, the results suggested that si-EZR-AS1 inhibited SCC13 and SCL-1 cell viability and proliferation.

si-EZR-AS1 inhibits cSCC cell migration and invasion, and promotes apoptosis. To investigate the role of EZR-AS1 in cSCC cell migration, invasion and apoptosis, wound healing, Transwell invasion and flow cytometry assays were performed, respectively. At 48 h, the relative wound width of the si-EZR-AS1-1 group was significantly increased compared with the si-NC group in both SCC13 and SCL-1 cells (P<0.01; Fig. 3A). Compared with the pc-NC group, the relative wound width was significantly decreased in the pc-EZR-AS1 group in A431 cells (P<0.01; Fig. 3B). The Transwell invasion assay results indicated that compared with the si-NC group, the number of invading cells in the si-EZR-AS1-1 group was significantly decreased in SCC13 and SLC-1 cells (P<0.01; Fig. 3C). In A431 cells, the number of invading cells in the pc-EZR-AS1 group was significantly increased compared with the pc-NC group (P<0.01; Fig. 3D). The flow cytometry results demonstrated that EZR-AS1 knockdown significantly increased the rate of apoptosis in SCC13 and SCL-1 cells compared with the si-NC group, whereas EZR-AS1 overexpression significantly decreased the rate of apoptosis in A431 cells compared with the pc-NC group (P<0.01; Fig. 4). Collectively, the results indicated that EZR-AS1 knockdown inhibited cSCC cell migration and invasion, and promoted cell apoptosis.

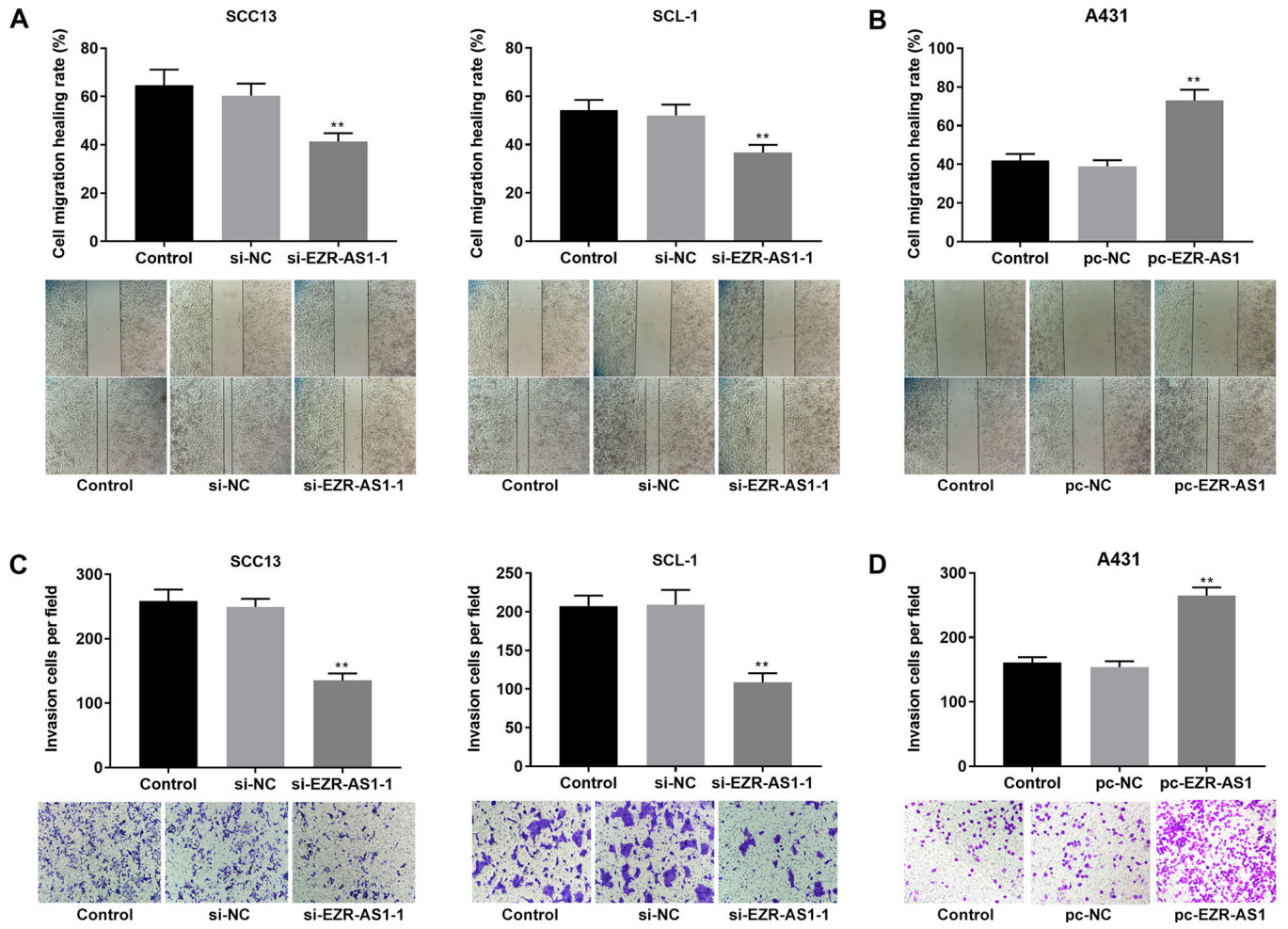

Figure 3. si-EZR-AS1inhibits cutaneous squamous cell carcinoma cell migration and invasion. The wound healing assay was performed to assess (A) SCC13, SCL-1 and (B) A431 cell migration. Scale bar, 100 μm. A Transwell invasion assay was performed to assess (C) SCC13, SCL-1 and (D) A431 cell invasion (magnification, x200). **P<0.01 vs. si-NC or pc-NC. si, small interfering RNA; EZR-AS1, ezrin antisense RNA 1; NC, negative control.

si-EZR-AS1 downregulates MMP-2, MMP-9 and Bcl-2 protein expression levels, and increases Bax protein expression in cSCC cells. MMP-2 and MMP-9 belong to the MMP family and serve an important role in tumor cell invasion and migration (28), whereas Bax and Bcl-2 belong to the Bcl-2 family and are two important factors that regulate apoptosis (29). Western blotting was performed to detect protein expression levels. Compared with the si-NC group, EZR-AS1 knockdown significantly reduced the protein expression levels of MMP-2, MMP-9 and Bcl-2, but significantly increased the protein expression levels of Bax (P<0.01; Fig. 5A and B). Compared with the pc-NC group, EZR-AS1 overexpression significantly increased the protein expression levels of MMP-2, MMP-9 and Bcl-2, and significantly reduced the protein expression levels of Bax (P<0.01; Fig. 5C). The results suggested that EZR-AS1 knockdown decreased the protein expression levels of MMP-2, MMP-9 and Bcl-2 and increased Bax protein expression levels.

si-EZR-AS1 inhibits the PI3K/AKT signaling pathway in cSCC cells. PI3K/AKT is a classic signaling pathway that is often overexpressed in cancer cells (30). To further explore the mechanism underlying EZR-AS1 in cSCC progression, western blotting was performed to detect the effect of EZR-AS1 on the PI3K/AKT signaling pathway. Compared with the si-NC group, EZR-AS1 knockdown significantly decreased the protein expression levels of p-PI3K/PI3K and p-AKT/AKT in SCC13 and SCL-1 cells (P<0.001; Fig. 6A and B). By contrast, compared with the pc-NC group, EZR-AS1 overexpression significantly increased the protein expression levels of p-PI3K/PI3K and p-AKT/AKT in A431 cells (P<0.01; Fig. 6C). FAK is a critical gene that regulates the PI3K/AKT signaling pathway (31). The analysis of LncTar identified FAK as a target of EZR-AS1 (Fig. 6D). The RIP assay results verified the target relationship between EZR-AS1 and FAK (Fig. 6E). The western blotting results demonstrated that EZR-AS1 knockdown significantly decreased the expression levels of FAK compared with the si-NC group (P<0.01; Fig. 6F). Furthermore, the RT-qPCR results suggested that FAK expression was significantly higher in cSCC tissues compared with healthy tissues (P<0.01; Fig. 6G). To confirm the regulatory effect of EZR-AS1 and FAK on the PI3K/AKT signaling pathway, the protein expression levels of p-PI3K/PI3K and p-AKT/AKT in SCC13 and SCL-1 cells were measured following co-transfection with si-EZR-AS1-1 and pc-FAK. FAK protein expression levels in the pc-FAK group were significantly higher compared with the pc-NC group (P<0.01; Fig. 6H). Compared with the pc-NC group, the protein expression levels of p-PI3K/PI3K and p-AKT/AKT in the pc-FAK

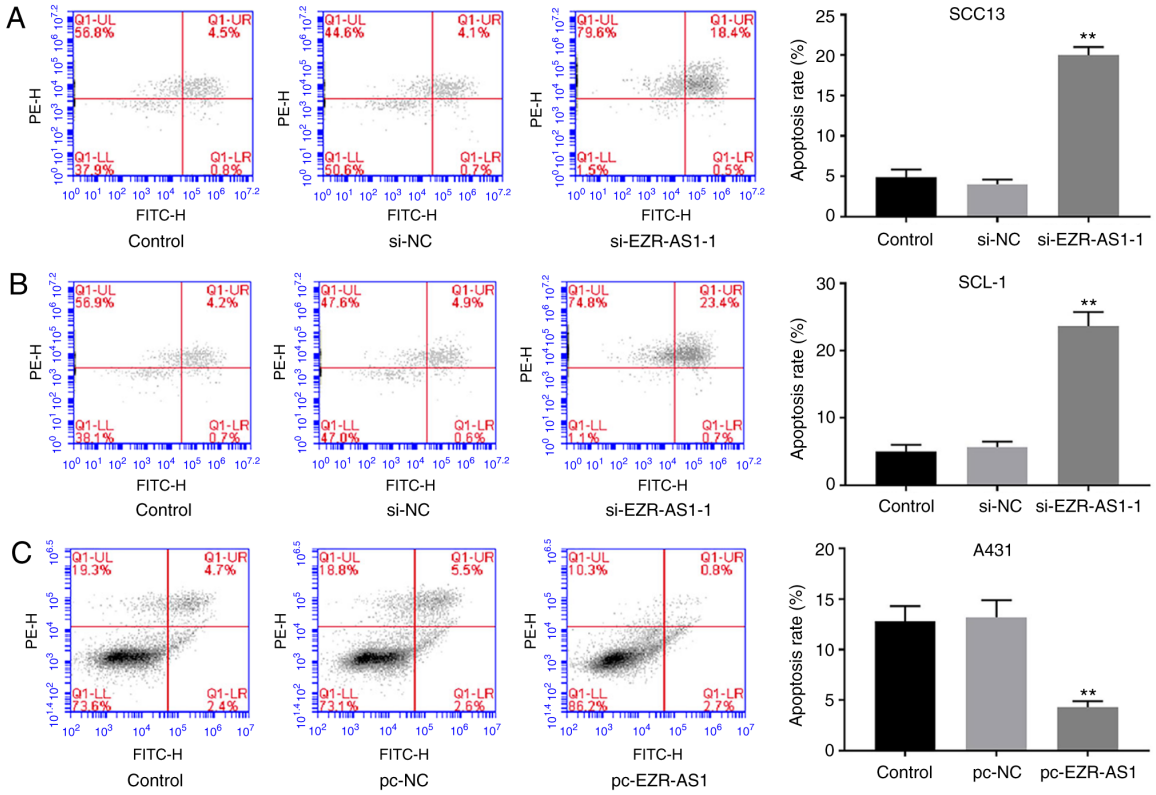

Figure 4. si-EZR-AS1 promotes cutaneous squamous cell carcinoma cell apoptosis. Flow cytometry was performed to detect (A) SCC13, (B) SCL-1 and (C) A431 cell apoptosis. **P<0.01 vs. si-NC or pc-NC. si, small interfering RNA; EZR-AS1, ezrin antisense RNA 1; NC, negative control.

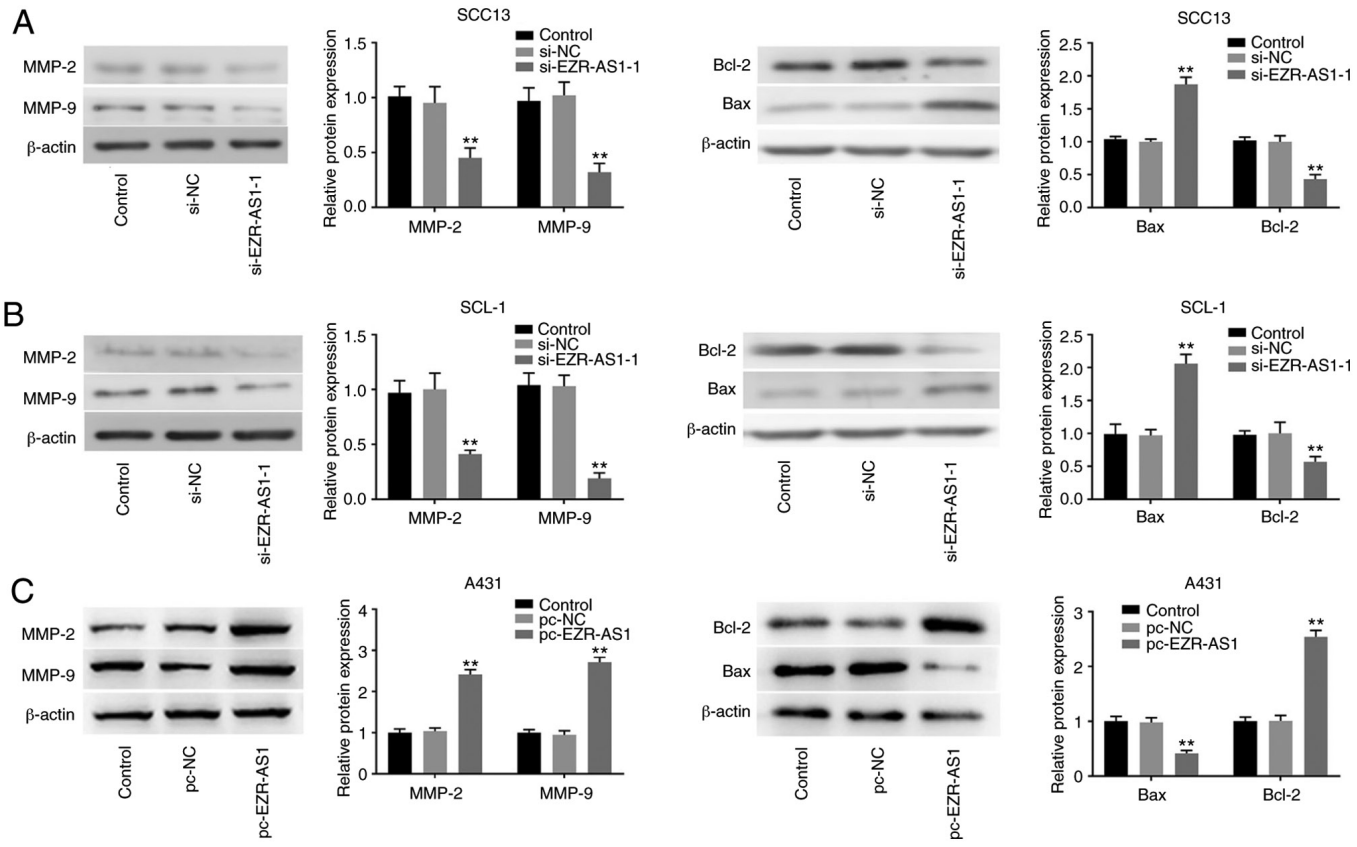

Figure 5. si-EZR-AS1 downregulates the protein expression levels of MMP-2, MMP-9 and Bcl-2, and increases Bax protein expression levels in cutaneous squamous cell carcinoma cells. Western blotting was performed to measure the protein expression levels of MMP-2, MMP-9, Bax and Bcl-2 in (A) SCC13, (B) SCL-1 and (C) A431 cells. **P<0.01 vs. si-NC or pc-NC. si, small interfering RNA; EZR-AS1, ezrin antisense RNA 1; MMP, matrix metallopeptidase; NC, negative control.

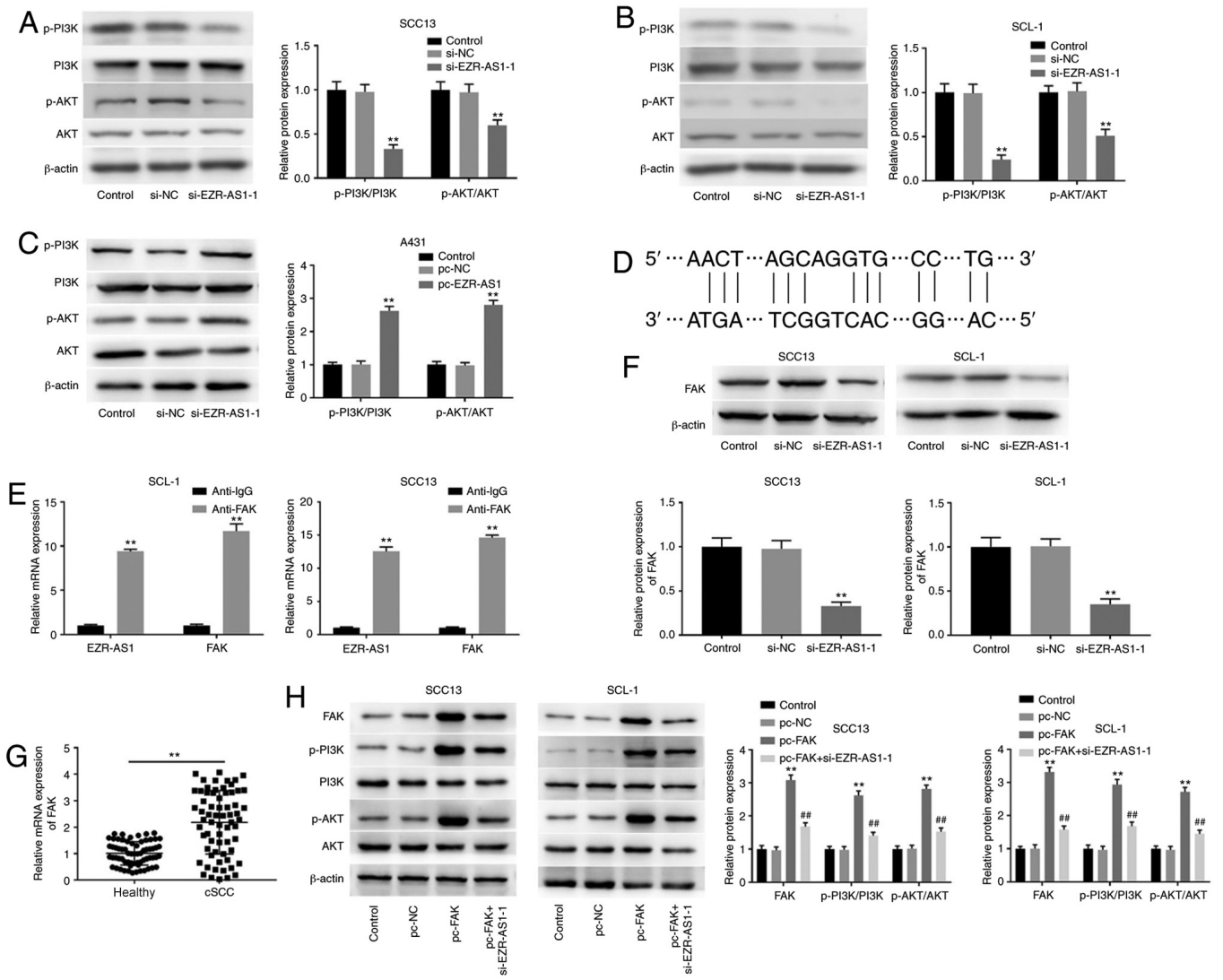

Figure 6. si-EZR-AS1 inhibits the PI3K/AKT signaling pathway in cSCC cells. Western blotting was performed to measure the protein expression levels of p-PI3K/PI3K and p-AKT/AKT in (A) SCC13, (B) SCL-1 and (C) A431 cells. (D) LncTar analysis identified FAK as a target of EZR-AS1. (E) The RNA immunoprecipitation assay was performed to confirm FAK as a target of EZR-AS1. (F) Effect of EZR-AS1 knockdown on FAK protein expression levels in SCC13 and SCL-1 cells. (G) FAK mRNA expression levels in cSCC tissues and healthy adjacent tissues. (H) Western blotting was performed to measure the protein expression levels of FAK, p-PI3K/PI3K and p-AKT/AKT in pc-FAK- and si-EZR-AS1-1-transfected SCC13 and SLC-1 cells. **P<0.01 vs. si-NC, pc-NC, anti-IgG or healthy; $^{\#\#}$P<0.01 vs. pc-FAK. si, small interfering RNA; EZR-AS1, ezrin antisense RNA 1; cSCC, cutaneous squamous cell carcinoma; p, phosphorylated; FAK, focal adhesion kinase; NC, negative control.

group were significantly increased in SCC13 and SCL-1 cells (P<0.01; Fig. 6H). However, the effects of FAK overexpression on FAK, p-PI3K/PI3K and p-AKT/AKT expression levels were significantly reversed by EZR-AS1 knockdown (P<0.01; Fig. 6H). In summary, EZR-AS1 knockdown inhibited the PI3K/AKT signaling pathway by suppressing FAK expression in cSCC cells.

EZR-AS1 affects cSCC cell proliferation, migration, invasion and apoptosis via the PI3K/AKT signaling pathway. To further investigate the relationship between EZR-AS1 and the PI3K/AKT signaling pathway in cSCC progression, 740Y-P (a PI3K agonist) was used. Compared with the control group, 740Y-P significantly increased the expression levels of p-AKT/AKT and p-PI3K/PI3K, and significantly reversed si-EZR-AS1-1-mediated effects on p-AKT/AKT and p-PI3K/PI3K expression levels (all P<0.01; Fig. 7A). Compared with the control group, EZR-AS1 knockdown significantly reduced colony formation, whereas 740Y-P significantly reversed the inhibitory effects of si-EZR-AS1 on SCC13 cell colony formation (all P<0.01; Fig. 7B). Similarly, 740Y-P significantly reversed si-EZR-AS1-mediated effects on SCC13 cell migration, invasion and apoptosis (P<0.01; Fig. 7C-E). Collectively, the aforementioned results indicated that EZR-AS1 knockdown inhibited cSCC cell proliferation, migration and invasion, and promoted cSCC cell apoptosis via inhibiting the PI3K/AKT signaling pathway.

Discussion

In recent years, lncRNAs have been reported to regulate various cellular processes, including cell proliferation, metastasis, differentiation and metabolism, leading to the progression of numerous diseases, including malignant tumors (32).

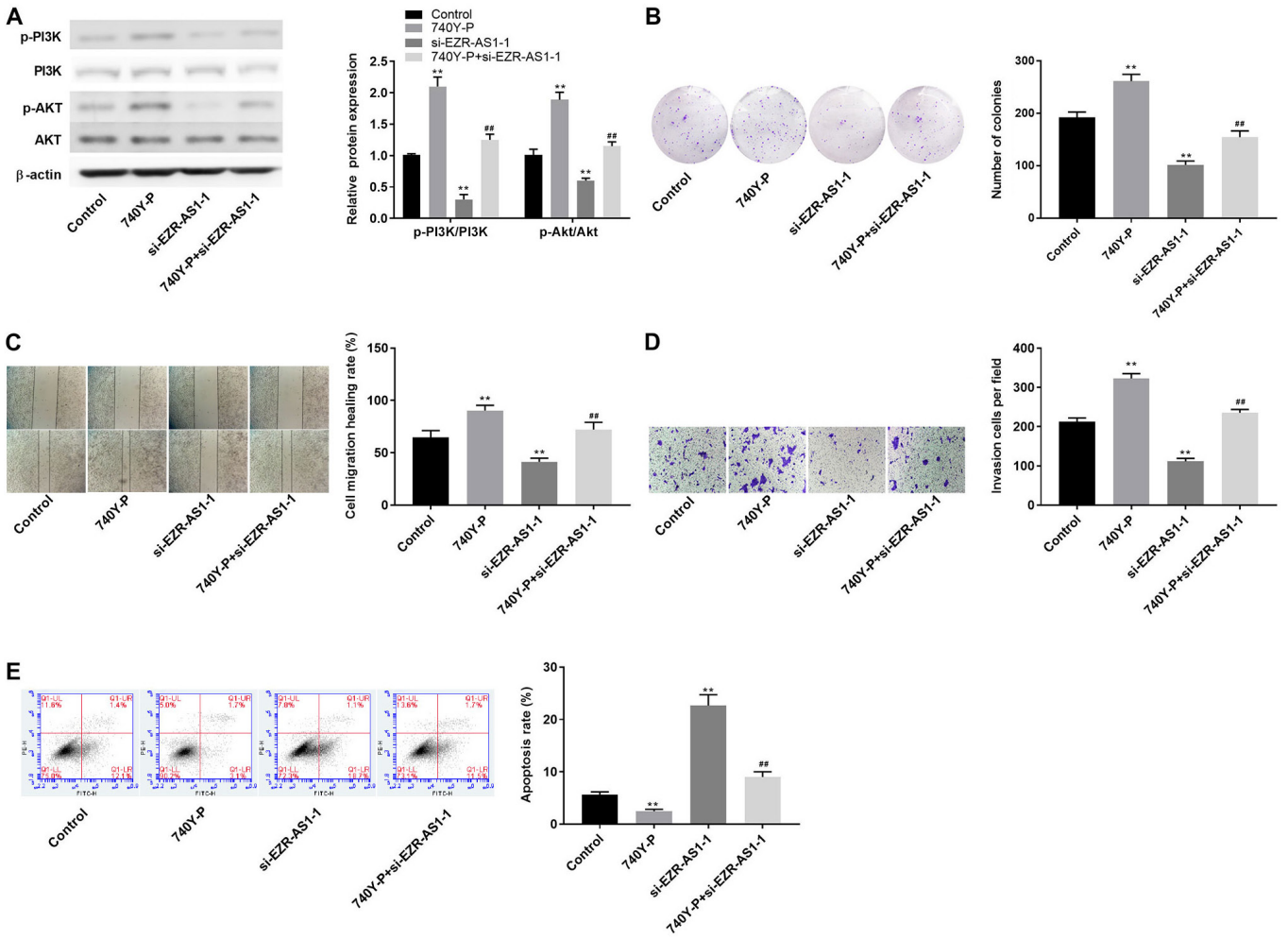

Figure 7. EZR-AS1 regulates cutaneous squamous cell carcinoma cell proliferation, migration, invasion and apoptosis via the PI3K/AKT signaling pathway. (A) Western blotting was performed to assess the effect of 740Y-P on the protein expression levels of p-AKT/AKT and p-PI3K/PI3K. (B) The effect of 740Y-P on SCC13 cell colony formation was assessed by performing the plate cloning assay (magnification, x40). The effect of 740Y-P on SCC13 cell migration and invasion was assessed by performing (C) wound healing (scale bar, 100 μm) and (D) Transwell invasion (magnification, x200) assays, respectively. (E) The effect of 740Y-P on SCC13 cell apoptosis was determined by performing flow cytometry. **P<0.01 vs. control or si-NC; $^{\#\#}$P<0.01 vs. si-EZR-AS1-1. EZR-AS1, ezrin antisense RNA 1; p, phosphorylated; si, small interfering RNA; NC, negative control.

In the present study, lncRNA EZR-AS1 expression was significantly upregulated in cSCC cells compared with HaCaT cells. In addition, compared with the si-NC group, EZR-AS1 knockdown significantly inhibited SCC13 and SCL-1 cell proliferation, migration and invasion, and promoted cell apoptosis. Mechanistically, the results indicated that lncRNA EZR-AS1 might exert its molecular function via the PI3K/AKT signaling pathway, thus affecting cSCC progression.

lncRNA EZR-AS1 is a key regulator of disease progression in numerous types of cancer, including ESCC, breast cancer and colorectal cancer, but the biological function of EZR-AS1 is not completely understood (15,20,21). A previous study have demonstrated that lncRNA EZR-AS1 knockdown can inhibit TGF-β signaling, thereby inhibiting colorectal cancer cell proliferation, invasion, migration and epithelial-mesenchymal transition, and promoting apoptosis (15). In addition, EZR-AS1 knockdown significantly inhibited ESCC cell migration, reduced tumor volume and weight, and reduced the number of metastatic lymph nodes in mice (21). The specific regulatory effects and mechanisms underlying lncRNA EZR-AS1 in cSCC are not completely understood. In the present study, EZR-AS1 expression was significantly increased in cSCC cells compared with HaCaT cells. Compared with the si-NC group, EZR-AS1 knockdown significantly inhibited SCC13 and SCL-1 cell proliferation, migration and invasion, and induced apoptosis. Moreover, EZR-AS1 targeted FAK in cSCC cells. Moreover, compared with the si-NC group, EZR-AS1 knockdown significantly decreased FAK expression, and FAK expression levels were significantly higher in cSCC tissues compared with healthy tissues.

The basic features of the metastasis process include tumor cell invasion and migration (33). In recent years, MMPs have been considered as important proteases related to tumor invasion and migration, especially the two metal proteins, MMP-2 and MMP-9 (28). MMP-2 and MMP-9 promote the progression of ovarian cancer, and their expression level increases with the increased malignant potential of ovarian tumors (34). In addition, Li *et al* (35) also reported that MMP-2/MMP-9 induction promoted hepatocellular carcinoma cell metastasis. Consistently, the present study demonstrated that EZR-AS1 knockdown significantly decreased MMP-2 and MMP-9 protein expression levels compared with the si-NC group.

Apoptosis is regulated by specific proteins, which regulates tumorigenesis and development (36). Among the specific apoptosis-related proteins, Bax can promote cancer cell apoptosis, whereas Bcl-2 can interact with Bax to regulate the occurrence of apoptosis (29). The present study demonstrated that EZR-AS1 knockdown significantly upregulated Bax expression and significantly downregulated Bcl-2 expression compared with the si-NC group. Collectively, the results indicated that EZR-AS1 may serve as an oncogene and contribute to cSCC malignancy.

PI3K/AKT is an important intracellular signaling pathway directly related to cell dormancy, proliferation, canceration and longevity (37). PI3K is a downstream mediator of the cell membrane tyrosine kinase receptor, which can phosphorylate phosphatidylinositol 4,5-bisphosphate to form phosphatidylinositol [3-5]-triphosphate. PIP3 activates the serine/threonine kinase AKT, which regulates cellular functions by phosphorylating downstream factors, including various enzymes, kinases and transcription factors (38,39). An increasing number of studies have demonstrated that the PI3K/AKT signaling pathway serves a critical role in cSCC cell survival (25,40), and alterations in the molecular function of the signaling pathway primarily involves phosphorylation of PI3K and AKT (22). In the present study, the expression levels of p-PI3K/PI3K and p-AKT/AKT were significantly reduced by EZR-AS1 knockdown compared with the si-NC group. As the key regulator of the PI3K/AKT signaling pathway, FAK overexpression significantly increased the protein expression levels of p-PI3K/PI3K and p-AKT/AKT in cSCC cells compared with the pc-NC group. However, EZR-AS1 knockdown partly reversed FAK overexpression-mediated effects on the PI3K/AKT signaling pathway. To further investigate the relationship between EZR-AS1 and the PI3K/AKT signaling pathway in cSCC progression, 740Y-P (a PI3K agonist) was used. Compared with the control group, 740Y-P significantly increased the expression levels of p-AKT/AKT and p-PI3K/PI3K, and reversed si-EZR-AS1-mediated effects on the expression levels of p-AKT/AKT and p-PI3K/PI3K. Moreover, 740Y-P partially reversed the inhibitory effect of si-EZR-AS1 on SCC13 cell proliferation. Similarly, SCC13 cell migration, invasion and apoptosis were assessed, and the results indicated that 740Y-P reversed si-EZR-AS1-mediated effects on SCC13 cells.

To conclude, the present study demonstrated that EZR-AS1 was upregulated in cSCC cells compared with HaCaT cells. Furthermore, si-EZR-AS1 inhibited cSCC cell proliferation, migration and invasion, and promoted cell apoptosis compared with the si-NC group. The molecular mechanisms underlying EZR-AS1 might be associated with the PI3K/AKT signaling pathway. The results provided novel insights into the diagnosis and treatment of cSCC.

Acknowledgements

Not applicable.

Funding

This study was supported by the National Natural Science Foundation of China (grant no. 81602756), the National Natural Science Foundation of Shan Dong University (grant no. ZR2016HQ37) and the Jinan Science and Technology Bureau of Shandong Province (grant no. 201821053).

Availability of data and materials

The datasets used and/or analyzed during the current study are available from the corresponding author on reasonable request

Authors' contributions

DL, LS and ZL performed the experiments. ZM provided technical support. DL and ZM analyzed the data and revised the manuscript. All authors read and approved the final manuscript.

Ethics approval and consent to participate

The present study was approved by the Ethics Committee of The Second Affiliated Hospital of Shandong First Medical University (approval no. 2020-181; Tai'an, China). All patients provided written informed consent.

Patient consent for publication

Not applicable.

Competing interests

The authors declare that they have no competing interests.

References

1. Liu S, Chen M, Li P, Wu Y, Chang C, Qiu Y, Cao L, Liu Z and Jia C: Ginsenoside rh2 inhibits cancer stem-like cells in skin squamous cell carcinoma. Cell Physiol Biochem 36: 499-508, 2015.
2. Ou C, Liu H, Ding Z and Zhou L: Chloroquine promotes gefitinib-induced apoptosis by inhibiting protective autophagy in cutaneous squamous cell carcinoma. Mol Med Rep 20: 4855-4866, 2019.
3. Mei XL and Zhong S: Long noncoding RNA LINC00520 prevents the progression of cutaneous squamous cell carcinoma through the inactivation of the PI3K/Akt signaling pathway by downregulating EGFR. Chin Med J (Engl) 132: 454-465, 2019.
4. Toll A, Gimeno-Beltrán J, Ferrandiz-Pulido C, Masferrer E, Yébenes M, Jucglà A, Abal L, Martí RM, Sanmartín O, Baró T, *et al*: D2-40 immunohistochemical overexpression in cutaneous squamous cell carcinomas: A marker of metastatic risk. J Am Acad Dermatol 67: 1310-1318, 2012.
5. Li Y, Huang C and Yang X: Characterization of TCF4-mediated oncogenic role in cutaneous squamous cell carcinoma. Int J Clin Exp Pathol 12: 3583-3594, 2019.
6. Ci C, Wu C, Lyu D, Chang X, He C, Liu W, Chen L and Ding W: Downregulation of kynureninase restrains cutaneous squamous cell carcinoma proliferation and represses the PI3K/AKT pathway. Clin Exp Dermatol 45: 194-201, 2020.
7. Burton KA, Ashack KA and Khachemoune A: Cutaneous squamous cell carcinoma: A review of high-risk and metastatic disease. Am J Clin Dermatol 17: 491-508, 2016.
8. Zilberg C, Lee MW, Kraitsek S, Ashford B, Ranson M, Shannon K, Iyer NG, Ch'ng S, Low TH, Palme C, *et al*: Is high-risk cutaneous squamous cell carcinoma of the head and neck a suitable candidate for current targeted therapies? J Clin Pathol 73: 17-22, 2020.
9. Uszczynska-Ratajczak B, Lagarde J, Frankish A, Guigo R and Johnson R: Towards a complete map of the human long non-coding RNA transcriptome. Nat Rev Genet 19: 535-548, 2018.

10. Shi D, Zhang C and Liu X: Long noncoding RNAs in cervical cancer. J Cancer Res Ther 14: 745-753, 2018.
11. Hosseini ES, Meryet-Figuiere M, Sabzalipoor H, Kashani HH, Nikzad H and Asemi Z: Dysregulated expression of long noncoding RNAs in gynecologic cancers. Mol Cancer 16: 107, 2017.
12. Chen L, Yao H, Wang K and Liu X: Long Non-coding RNA MALAT1 regulates ZEB1 expression by sponging miR-143-3p and promotes hepatocellular carcinoma progression. J Cell Biochem 118: 4836-4843, 2017.
13. Wang Y, Fu L, Sun A, Tang D, Xu Y, Li Z, Chen M and Zhang G: C/EBPβ contributes to transcriptional activation of long non-coding RNA NEAT1 during APL cell differentiation. Biochem Biophys Res Commun 499: 99-104, 2018.
14. Anastasiadou E, Jacob LS and Slack FJ: Non-coding RNA networks in cancer. Nat Rev Cancer 18: 5-18, 2018.
15. Liu Z, Wang N, Wang F, Zhang S and Ding J: Silencing of lncRNA EZR-AS1 inhibits proliferation, invasion, and migration of colorectal cancer cells through blocking transforming growth factor β signaling. Biosci Rep 39: BSR20191199, 2019.
16. You G, Long X, Song F, Huang J, Tian M, Xiao Y, Deng S and Wu Q: Long noncoding RNA EZR-AS1 regulates the proliferation, migration, and apoptosis of human venous endothelial cells via SMYD3. Biomed Res Int 2020: 6840234, 2020.
17. Ghaffari A, Hoskin V, Turashvili G, et al: Intravital imaging reveals systemic ezrin inhibition impedes cancer cell migration and lymph node metastasis in breast cancer. Breast Cancer Res 21: 12, 2019.
18. Xie JJ, Xu LY, Wu ZY, Zhao Q, Xu XE, Wu JY, Huang Q and Li EM: Prognostic implication of ezrin expression in esophageal squamous cell carcinoma. J Surg Oncol 104: 538-543, 2011.
19. Xie YH, Li LY, He JZ, Xu XE, Liao LD, Zhang Q, Xie JJ, Xu LY and Li EM: Heat shock protein family B member 1 facilitates ezrin activation to control cell migration in esophageal squamous cell carcinoma. Int J Biochem Cell Biol 112: 79-87, 2019.
20. Bai Y, Zhou X, Huang L, Wan Y, Li X and Wang Y: Long noncoding RNA EZR-AS1 promotes tumor growth and metastasis by modulating Wnt/β-catenin pathway in breast cancer. Exp Thera Med 16: 2235-2242, 2018.
21. Zhang XD, Huang GW, Xie YH, He JZ, Guo JC, Xu XE, Liao LD, Xie YM, Song YM, Li EM and Xu LY: The interaction of lncRNA EZR-AS1 with SMYD3 maintains overexpression of EZR in ESCC cells. Nucleic Acids Res 46: 1793-1809, 2018.
22. Polivka J Jr and Janku F: Molecular targets for cancer therapy in the PI3K/AKT/mTOR pathway. Pharmacol Ther 142: 164-175, 2014.
23. Gou XJ, Bai HH, Liu LW, Chen HY, Shi Q, Chang LS, Ding MM, Shi Q, Zhou MX, Chen WL and Zhang LM: Asiatic acid interferes with invasion and proliferation of breast cancer cells by inhibiting WAVE3 activation through PI3K/AKT signaling pathway. Biomed Res Int 2020: 1874387, 2020.
24. Li C, Qin Y, Zhong Y, Qin Y, Wei Y, Li L and Xie Y: Fentanyl inhibits the progression of gastric cancer through the suppression of MMP-9 via the PI3K/Akt signaling pathway. Ann Transl Med 8: 118, 2020.
25. Troiano A, Lomoriello IS, di Martino O, Fusco S, Pollice A, Vivo M, La Mantia G and Calabro V: Y-box binding protein-1 is part of a complex molecular network linking ΔNp63α to the PI3K/akt pathway in cutaneous squamous cell carcinoma. J Cell Physiol 230: 2067-2074, 2015.
26. Livak KJ and Schmittgen TD: Analysis of relative gene expression data using real-time quantitative PCR and the 2(-Delta Delta C(T)) method. Methods 25: 402-408, 2001.
27. Cao Z, Pan X, Yang Y, Huang Y and Shen HB: The lncLocator: A subcellular localization predictor for long non-coding RNAs based on a stacked ensemble classifier. Bioinformatics 34: 2185-2194, 2018.
28. Li X, Bao C, Ma Z, Xu B, Ying X, Liu X and Zhang X: Perfluorooctanoic acid stimulates ovarian cancer cell migration, invasion via ERK/NF-κB/MMP-2/-9 pathway. Toxicol Lett 294: 44-50, 2018.
29. Jarskog LF, Selinger ES, Lieberman JA and Gilmore JH: Apoptotic proteins in the temporal cortex in schizophrenia: High Bax/Bcl-2 ratio without caspase-3 activation. Am J Psychiatry 161: 109-115, 2004.
30. Sathe A and Nawroth R: Targeting the PI3K/AKT/mTOR pathway in bladder cancer. Methods Mol Biol 1655: 335-350, 2018.
31. Zhang SL, Ma L, Zhao J, You SP, Ma XT, Ye XY and Liu T: The phenylethanol glycoside liposome inhibits PDGF-induced HSC activation via regulation of the FAK/PI3K/Akt signaling pathway. Molecules 24: 3282, 2019.
32. Duan H, Li X, Chen Y, Wang Y and Li Z: LncRNA RHPN1-AS1 promoted cell proliferation, invasion and migration in cervical cancer via the modulation of miR-299-3p/FGF2 axis. Life Sci 239: 116856, 2019.
33. Liao CL, Chu YL, Lin HY, Chen CY, Hsu MJ, Liu KC, Lai KC, Huang AC and Chung JG: Bisdemethoxycurcumin suppresses migration and invasion of human cervical cancer HeLa cells via inhibition of NF-kB, MMP-2 and -9 pathways. Anticancer Res 38: 3989-3997, 2018.
34. Rasool M, Malik A, Basit Ashraf MA, Parveen G, Iqbal S, Ali I, Qazi MH, Asif M, Kamran K, Iqbal A, *et al*: Evaluation of matrix metalloproteinases, cytokines and their potential role in the development of ovarian cancer. PLoS One 11: e0167149, 2016.
35. Li X, Yang Z, Song W, *et al*: Overexpression of Bmi-1 contributes to the invasion and metastasis of hepatocellular carcinoma by increasing the expression of matrix metalloproteinase (MMP)-2, MMP-9 and vascular endothelial growth factor via the PTEN/PI3K/Akt pathway. Int J Oncol 43: 793-802, 2013.
36. Pistritto G, Trisciuoglio D, Ceci C, Garufi A and D'Orazi G: Apoptosis as anticancer mechanism: Function and dysfunction of its modulators and targeted therapeutic strategies. Aging (Albany NY) 8: 603-619, 2016.
37. Zhu F, Jiang D, Zhang M and Zhao B: 2,4-Dihydroxy-3'-methoxy-4'-ethoxychalcone suppresses cell proliferation and induces apoptosis of multiple myeloma via the PI3K/akt/mTOR signaling pathway. Pharm Biol 57: 641-648, 2019.
38. Sanz Ressel BL, Massone AR and Barbeito CG: Immunohistochemical expression of selected phosphoproteins of the mTOR signalling pathway in canine cutaneous squamous cell carcinoma. Vet J 245: 41-48, 2019.
39. Wu XY, Tian F, Su MH, Wu M, Huang Y, Hu LH, Jin L and Zhu XJ: BF211, a derivative of bufalin, enhances the cytocidal effects in multiple myeloma cells by inhibiting the IL-6/JAK2/STAT3 pathway. Int Immunopharmacol 64: 24-32, 2018.
40. Yao M, Shang YY, Zhou ZW, Yang YX, Wu YS, Guan LF, Wang XY, Zhou SF and Wei X: The research on lapatinib in autophagy, cell cycle arrest and epithelial to mesenchymal transition via Wnt/ErK/PI3K-AKT signaling pathway in human cutaneous squamous cell carcinoma. J Cancer 8: 220-226, 2017.